Banknote Image Retrieval Using Rotated Quaternion Wavelet Filters

Shan Gai [1] Peng Liu [1] , Jiafeng Liu [1] , Xianglong Tang [1]

[1] *Computer Science and Technology, Harbin Institute of Technology, NanGang District and XiDaZhi street No.92, Harbin, 150001, China*

E-mail: gaishan886@163.com
E-mail: egami@126.com
E-mail: jefferyliu@hit.edu.cn
E-mail: tangxl@hit.edu.cn

Received: 27-06-2010
Accepted: 22-11-2010

Abstract

A new method of banknote image retrieval is proposed by using new set of rotated quaternion wavelet filters (RQWF) and standard quaternion wavelet transform (QWT) jointly. The robust and rotationally invariant features are extracted from QWT and RQWF decomposed sub-bands of banknote image. Three different sets of databases are used to demonstrate the effectiveness of the proposed method. The experimental results show that the proposed method improves the recognition rate from 78.79% to 91.22% on (16000 images) database D1, form 74.08% to 94.62% on (20000 images) database D2 and from 76.44% to 88.78% on (10000 images) database D3. The proposed method can also obtain a reasonable level of computational complexity.

Keywords: discrete wavelet transform (DWT), complex wavelet transform (CWT), quaternion wavelet transform (QWT), rotated quaternion wavelet filters (RQWF), feature extraction, support vector machine (SVM).

1. Introduction

With the development of modern science,the banknote recognition system becomes more and more important.The goal of the system is to sort the banknotes according to their value and face automatically. Feature extraction and classification are very important components in banknote recognition system.

Several authors have proposed many feature extraction methods.Liu and Picard [1] used wold features for image modeling and retrieval. Manjunath and Ma [2] used Gabor wavelet coefficients for image retrieval.Discrete wavelet transform (DWT) [3-8] was proposed for image feature extraction.Do and Vetterli[9] proposed wavelet based texture retrieval by the use of generalized Gaussian density and Kullback-Leibler distance metric.A comparative study of rotation invariant texture analysis method was proposed by Janney et al [10].Magnitude of a discrete Fourier transform in the rotation dimension of features obtained with a multi-resolution [11-12].Chen [13] modeled the features of wavelet sub-band as a hid-

den Markov model (HMM).In [14],Manthalkar presented rotation-invariant texture features using a wavelet packet transform.The real DWT has two drawbacks of shift sensitivity and poor directionality [15].Selesnick and Kingsbury [16]proposed DT-CWT which can represent image texture efficiently in six directions.Also,reference [17] obtained improved retrieval performance by the use of DT-CWT. But DT-CWT is a single phase, which can't resolve the image shift in both the horizontal and vertical directions from the change of only one CWT coefficient phase.

The new quaternion wavelet transform (QWT) [18-19] was proposed in recent years for overcoming drawbacks of DWT and DT-CWT.The QWT can provide three phases for image analysis by using the phase concept.QWT used the Gabor kernel as quaternion mother wavelet,and extended to multiresolution analysis.Different phases are computed in different resolutions by the modulated quaternion Gabor filters.

To improve the retrieval performance both in terms of retrieval accuracy and retrieval time, a new set of 2-D rotated quaternion wavelet filters is proposed in this paper.The proposed banknote image retrieval method combined QWT and RQWF is used in banknote recognition system. The method is checked on three sets of large databases and compared with existing available methods on corresponding databases. The performance of the proposed method is better than that of the existing available methods on each database.

This paper is organized as follows.Rotated quaternion wavelet filters are proposed in section 2. Section 3 provides an overview of support vector machine (SVM). The banknote image retrieval system using QWT+RQWF+SVM is proposed in section 4. Experimental results are given in section 5, which is followed by the conclusion in section 6.

2. Rotated Quaternion Wavelet

2.1. Real Wavelet Transform

The one-dimensional (1-D) discrete real wavelet transform decomposes signal $f(x)$ with dilated and shifted mother wavelet $\varphi(x)$ and scaling function $\phi(x)$.

$$f(x)=\sum_{l\in Z}A_{j_0,l}\phi_{j_0,l}(x)+\sum_{j=1}^{j_0}\sum_{l\in Z}D_{j,l}\varphi_{j,l}(x) \quad (1)$$

where the approximation coefficients $A_{j_0,l}$ and wavelet coefficients $D_{j,l}$ at scale j can be calculated using the standard inner product $A_{j_0,l}=\langle f,\phi_{j_0,l}\rangle$ and $D_{j,l}=\langle f,\varphi_{j,l}\rangle$, in which $\phi_{j_0,l}(x)=2^{\sqrt{j_0}}\phi\left(2^{j_0}x-l\right)$ and mother wavelet function $\varphi_{j,l}(x)=2^{\sqrt{j}}\varphi\left(2^{j}x-l\right)$.Given the approximation coefficients $A_{j,l}$ at scale j, then the approximation coefficients $A_{j+1,l}$ and wavelet coefficients $D_{j+1,l}$ at scale $j+1$ are obtained by passing $A_{j,l}$ through low-pass filter h and high-pass filter g.The operation of down-sampling is by a factor of two. The standard two-dimensional (2-D) wavelet transform is obtained using tensor products of 1-D wavelets transform over the vertical and horizontal directions. It decomposes the signal of image $f(x,y)$ in terms of a set of wavelet functions which are strongly oriented in $\{0^\circ,90^\circ,\pm45^\circ\}$ and scaling function.

$$f(x,y)=\sum_{l\in Z^2}A_{j_0,l}\phi_{j_0,l}(x,y)+\sum_{k\in\alpha}\sum_{j=1}^{j_0}\sum_{l\in Z^2}D^k_{j,l}\varphi^k_{j,l}(x,y) \quad (2)$$

where $\phi_{j_0,l}(x,y)=2^{j_0}\phi(2^{j_0}(x,y)-l)$ and $\varphi^k_{j,l}(x,y)=2^j\varphi^k(2^j(x,y)-l)$. The 2-D separable wavelet transform is constructed in terms of 2-D scaling and three 2-D wavelet functions as follows

$$\begin{aligned}\phi(x,y)&=\phi(x)\phi(y)\\ \varphi^0(x,y)&=\phi(x)\varphi(y)\\ \varphi^{90}(x,y)&=\varphi(x)\phi(y)\\ \varphi^{\pm45}(x,y)&=\varphi(x)\varphi(y)\end{aligned} \quad (3)$$

where ϕ,φ are 1-D scaling function and wavelet functions as described in (1).The 2-D real wavelet transform of three sub-bands is shown in Fig1.

Fig. 1. Impulse response of 2-D wavelet filters

2.2. Complex Wavelet Transform

The real DWT has two drawbacks. The first is shift variance which causes significant fluctuation in the wavelet coefficient energy. The second drawback is poor directional selectivity as shown in Fig 2. Complex wavelet transform (CWT) provide an avenue to remedy these two drawbacks.In CWT, the filters have complex coefficients and make the output samples are complex. However, it is difficult to achieve a perfect reconstruction for complex wavelet decomposition beyond level one.Selesnick and Kingsbury [11] proposed a method of DT-CWT which remedied this drawback of CWT.The DT-CWT is implemented by two parallel fully decimated trees with real filter and then combining sub-band coefficients appropriately.The 1-D DT-CWT decomposes a signal $f(x)$ in terms of scaling function and a set of complex shifted and dilated mother wavelet functions as follows.

$$f(x) = \sum_{l\in Z} A_{j_0,l}\phi_{j_0,l}(x) + \sum_{j=1}^{j_0}\sum_{l\in Z} D_{j,l}\varphi_{j,l}(x) \quad (4)$$

where $A_{j_0,l}$ and $D_{j,l}$ denote scaling coefficients and complex wavelet coefficients respectively. They are determined by $\phi_{j_0} = \phi^r_{j_0,l} + j\times\phi^i_{j_0,l}$ and $\varphi_{j,l} = \varphi^r_{j,l} + j\times\varphi^i_{j,l}$. Two real wavelet transform consists of complex wavelet transform. The real and imaginary parts of the DT-CWT are calculated using h_0,h_1 and g_0,g_1,which are separate wavelet filters.In 2-D DT-CWT, an image signal $f(x,y)$ is decomposed using a complex scaling function and six complex wavelet functions.

$$f(x,y) = \sum_{l\in Z^2} A_{j_0,l}\phi_{j_0,l}(x,y) + \sum_{k\in\alpha}\sum_{j=1}^{j_0}\sum_{l\in Z^2} D^k_{j,l}\varphi^k_{j,l}(x,y) \quad (5)$$

where $A_{j_0,l}$ and $D^k_{j,l}$ are scaling coefficients and wavelet coefficients respectively. $\phi_{j_0,l}(x,y)$ denotes the scaling function and $\varphi^k_{j,l}(x,y)$ denotes six wavelet functions which are oriented at $k\in\alpha = \{\pm15^\circ,\pm45^\circ,\pm75^\circ\}$.Minh[20] proposed a theorem that if $H_0(e^{j\omega})$ and $G_0(e^{j\omega})$ are low-pass conjugate quadrature filters as follows:

$$G_0(e^{j\omega}) = H_0(e^{j\omega})e^{-j0.5\omega} \quad (6)$$

the corresponding wavelets are a Hilbert transform pair denoted as $\varphi_g(x) = H\{\varphi_h(x)\}$.Then the 2-D DT-CWT is constructed by combining the two oriented non-separable 2-D wavelet transform.The directional wavelet function and scaling function are obtained by 2-D wavelet basis as follows:

$$\begin{aligned}\phi_1(x,y) &= \phi_h(x)\phi_h(y)\\ \phi_2(x,y) &= \phi_g(x)\phi_g(y)\end{aligned} \quad (7)$$

$$\begin{aligned}\varphi^{+15^\circ}(x,y) &= \varphi_1(x,y) = \phi_h(x)\varphi_h(y)\\ \varphi^{-15^\circ}(x,y) &= \varphi_2(x,y) = \phi_g(x)\varphi_g(y)\end{aligned} \quad (8)$$

$$\begin{aligned}\varphi^{+75^\circ}(x,y) &= \varphi_3(x,y) = \varphi_h(x)\phi_h(y)\\ \varphi^{-75^\circ}(x,y) &= \varphi_4(x,y) = \varphi_g(x)\phi_g(y)\end{aligned} \quad (9)$$

$$\begin{aligned}\varphi^{+45^\circ}(x,y) &= \varphi_5(x,y) = \varphi_h(x)\varphi_h(y)\\ \varphi^{-45^\circ}(x,y) &= \varphi_6(x,y) = \varphi_g(x)\varphi_g(y)\end{aligned} \quad (10)$$

The six complex wavelets are obtained by

$$\begin{aligned}\varphi_k(x,y) &= 2^{\sqrt{2}}(\varphi_k(x,y) + \varphi_{k+1}(x,y))\\ \varphi_{k+1}(x,y) &= 2^{\sqrt{2}}(\varphi_k(x,y) - \varphi_{k+1}(x,y))\end{aligned} \quad (11)$$

where $k = \{1,3,5\}$.The 2-D DT-CWT is implemented by taking sum and difference of two separable wavelet filter banks.The impulse response of six wavelets of DT-CWT is shown in Fig2. The DT-CWT are strongly oriented at six angles and can capture more image information than the conventional wavelet transform.

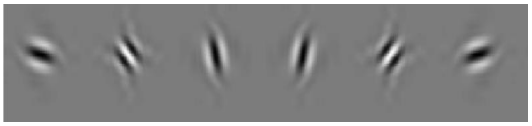

Fig. 2. Impulse response of 2-D DT-CWT filters

2.3. Quaternion Wavelet Transform

The 2-D DT-CWT can only capture the image features perpendicular to its orientation as it has a single phase.When the features oriented in both horizontal and vertical directions, it will cause ambiguity in the 2-D DT-CWT domain.Quaternion wavelet transform (QWT) can remedy this drawback. Each quaternion wavelet consists of a real part and three imaginary parts which are organized according to quaternion algebra.The quaternion algebra H is proposed by W.R.Hamiton in 1843.Given $Q = \{s + k_1a + k_2b + k_3c | s,a,b,c \in R\}$ has multiplication rules which are $k_1^2 = k_2^2 = k_3^2 = -1, k_3 = k_1k_2 = -k_2k_1$. Q^* which is conjugate of Q is defined as $Q^* = \{s - k_1a - k_2b - k_3c | s,a,b,c \in R\}$ and the magnitude is defined as $|Q| = \sqrt{QQ^*}$. Another way to represent a quaternion Q in a polar form as $Q = |Q|e^{k_1\alpha_1}e^{k_2\alpha_2}e^{k_3\alpha_3}$, where are the quaternion phase angles.They are calculated using the following formulas.

$$\alpha_1 = \frac{1}{2}\arctan\left(\frac{2(ac+sb)}{s^2+a^2-b^2-c^2}\right) \quad (12)$$

$$\alpha_2 = \frac{1}{2}\arctan\left(\frac{2(bc+sa)}{s^2-a^2+b^2-c^2}\right) \quad (13)$$

$$\alpha_3 = -\frac{1}{2}\arcsin\left(2(bc-ad)\right) \quad (14)$$

where $(\alpha_1,\alpha_2,\alpha_3) \in [-\pi,\pi] \cup [-\pi/2,\pi/2] \cup [-\pi/4,\pi/4]$.There are three nontrivial algebra involutions as follows.

$$T_1(Q) = -k_1Qk_1 = f(x,-y) \quad (15)$$

$$T_2(Q) = -k_2Qk_2 = f(x,-y) \quad (16)$$

$$T_3(Q) = -k_3Qk_3 = f(-x,-y) \quad (17)$$

where function $f : R^2 \rightarrow \mathrm{H}$ is called quaternion Hermitian for each (x,y). For image signal $f(x,y)$, the quaternion wavelet multi-resolution decomposition is defined as

$$f(x,y) = A_l^q f + \sum_{j=1}^{l}\left[D_{j,1}^q f + D_{j,2}^q f + D_{j,3}^q f\right] \quad (18)$$

where q denotes indication quaternion 2-D signal.$A_j^q f(x,y)$ is approximation function and $D_{j,p}^q f(x,y)(p = 1,2,3)$ is detail function which are computed by means of scaling function $\phi^q(x,y)$ and quaternion wavelet function $\varphi_p^q(x,y)$.We apply two wavelet filters h and g to each dimension of 2-D image signal.All possible combination of wavelet filters are hh, gg, hg, gh.They are applied to the 2-D image signal to generate four wavelet components oriented at horizontal, vertical and diagonal.The QWT coefficients are obtained using quaternion algebra by combing the wavelet components of the same sub-band from the filter bank.So the QWT wavelets at each scale can be organized as follows:

$$\mathrm{M} = \begin{bmatrix} \phi_h(x)\varphi_h(y) \\ \varphi_h(x)\phi_h(y) \\ \varphi_h(x)\varphi_h(y) \end{bmatrix} + k_1 \begin{bmatrix} \phi_g(x)\varphi_h(y) \\ \varphi_g(x)\phi_h(y) \\ \varphi_g(x)\varphi_h(y) \end{bmatrix} + k_2 \begin{bmatrix} \phi_h(x)\varphi_g(y) \\ \varphi_h(x)\phi_g(y) \\ \varphi_h(x)\varphi_g(y) \end{bmatrix} + k_3 \begin{bmatrix} \phi_g(x)\varphi_g(y) \\ \varphi_g(x)\phi_g(y) \\ \varphi_g(x)\varphi_g(y) \end{bmatrix} \quad (19)$$

2.4. Rotated Quaternion Wavelet Transform

The diagonal sub-band of the QWT is difficult to distinguish the information oriented in 45° or 135°.We propose new 2-D rotated quaternion wavelet filters (RQWF) to remedy this drawback.The new RQWF are oriented by rotating the non-separable quaternion wavelet filters using (19) by rotating the angle of 45° for each filters.So the decomposition is performed along the new directions.Let h and g represent 1-D high pass and low pass filter respectively.The size of filter is $(2N-1)\times(2N-1)$,where N is the length of filter.Given 2-D image signal $f(x,y)$,the 2-D RQWF is performed by using 2-D down-sampling operation.The set of RQWF has orthogonal property and the computational complexity of RQWF is the same as the QWT in the 2-D frequency domain.Fig3 illustrates the impulse response of RQWF which are strongly oriented in $\{45^\circ, 90^\circ, 135^\circ, 0^\circ\}$ correspond to $\{0^\circ, 45^\circ, 90^\circ, 135^\circ\}$ of QWT.From the Fig3, the

RQWF is obtained by rotating the filters of QWT the angle of 45°.As the characteristics of RQWF and QWT, it is possible to use them jointly in the image feature extraction. With rotated quaternion decomposition the diagonal characteristics in 45 and 135 degrees are clearly seen.An example of one level image decomposition using QWT and RQWF is shown in Fig4.

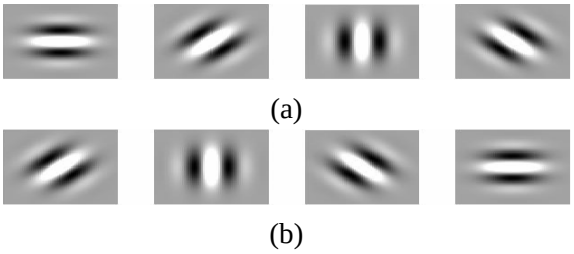

Fig. 3. Impulse response of 2-D QWT and RQWF, (a).2-D QWT filters with orientations: 0, 45, 90, 135 degrees. (b).2-D RQWF filters with orientations: 45, 90, 135, 0 degrees.

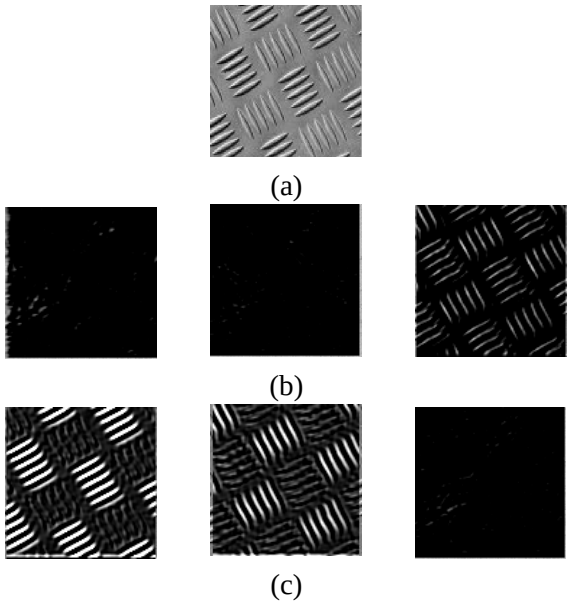

Fig. 4. One-level decomposition of texture image using QWT and RQWF,(a)Original image,(b)sub-bands using QWT (from left:0,-45,+45 and 90 degree),(c)sub-bands using RQWF (from left:45,0,90,135 degree)

3. Support Vector Machine

Classification is a common task in machine learning.Support vector machine (SVM) is one kind of classifier and it is based on strong foundations of the statistical learning theory.It is used in many applications such as face detection, character recognition,image classification and so on.Compared with other classifiers,there are many advantages, such as low computational complexity, better capacity of dealing with high dimensional data, less number of training data and robustness against noisy data.The goal of SVM which is a binary classifier can be represented as pairs of data denoted (x_i, y_i),where $x_i \in x^m, m$ is dimension of input space and $y_i \in \{-1, +1\}$ for the output classes.The linear classification function

$$f(x) = wX + b \tag{20}$$

where w, b denotes slope and intersection respectively. Fig5 illustrates the optimal and non-optimal hyper-planes of the SVM.

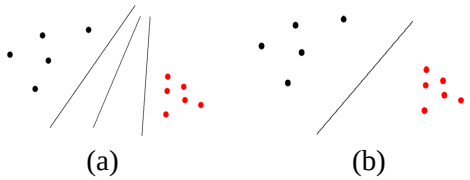

Fig. 5. Optimal and non-optimal hyper-planes,(a)various hyper-planes,(b)optimal hyper-plane

SVM can be extended for multi-class problem. It incorporates kernel functions for projecting of non-linearly separable input space to a higher dimension linearly separable space.There are many kernel functions, such as Gaussian, sigmoid, linear and radial bases functions.Multi-class problem includes one against all, one against one and all at once.Fig6 shows the process of grouping different classes in the banknote image database.Each SVM separates one class from the rest of the banknote images.

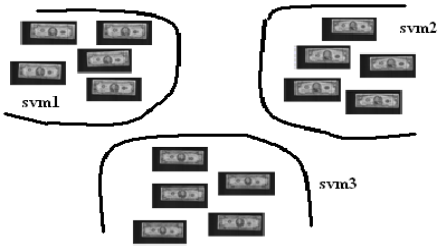

Fig. 6. One against all classification using three SVM

4. Banknote Image Retrieval System

4.1. Banknote Image Preprocessing

The process of preprocessing includes edge detection and slant correction.The edge detection is implemented by testing many dispersed points on the borders of the image and then adopt the least square method to fit the border line of the banknote image.As the banknote image samples are scanned in the movement,the geometric distortion occur to some extent.So slant correction is used to the banknote image for remedy the drawback.Fig7 and Fig8 show the process of the banknote image preprocessing.

(a) (b)

Fig. 7. Banknote image edge detection,(a)original image,(b)edge detection

(a) (b)

Fig. 8. Banknote image slant correction,(a)original image,(b)slant correction

4.2. Banknote Image Feature Extraction

Features are extracted from each banknote image in the image database using QWT and RQWF respectively.Five different sets of features are computed as follows.
(a).Feature Set1: DWT only.
(b).Feature Set2: DT-CWT only.
(c).Feature Set3: QWT only.
(d).Feature Set4: RQWF only.
(e).Feature Set5: QWT and RQWF.
The feature vector is constructed using energy and standard deviation.In each sub-band the feature vector is formed using the two parameter values.The motivation of using these features is that they are discriminated texture of the banknote image in the frequency domain.In the large banknote image database, the retrieval performance with combination of two features outperforms that using these two features individually. The energy and standard deviation of the kth sub-band is computed as follows:

$$E_k = \frac{1}{M \times N} \sum_{i=1}^{M} \sum_{j=1}^{N} |X_k(i,j)| \tag{21}$$

$$\sigma_k = \left[\frac{1}{M \times N} \sum_{i=1}^{M} \sum_{j=1}^{N} (X_k(i,j) - \mu_k) \right] \tag{22}$$

where $X_k(i,j)$ denotes the kth quaternion wavelet coefficients,$M \times N$ is the size of quaternion wavelet sub-band and μ_{ij} is the mean value of quaternion wavelet coefficients.The feature vector is formed using a combination of E_k and σ_k as follows $f = [\sigma_1, \sigma_2, \cdots, \sigma_k, E_1, E_2, \cdots, E_k]$.So the length of the vector is $2 \times k$.

4.3. Banknote Image Query Method

Some typical banknote image samples which belong to each class are selected for training using SVM.Considering the high speed and reliable performance, one against all training method is used in the experiment.The process is done by *trainlssvm* function of LSSVM. RBF is used as kernel function for the training SVM. LSSVM provides a function which can be used for overcoming the drawbacks of optimal parameter selection of SVM. In the experiment, grid search method is used for searching optimal parameters.Then the function *simlssvm* is used for computing the distance of each image included

in the database from each trained SVM is calculated. The distance vector store the distance of each image from each support vector machine.The correlation based metric can be used for comparison.

$$d_C(x_r, x_s) = \frac{(x_r - \mu_r)(x_s - \mu_s)'}{\sqrt{\left[(x_r - \mu_r)(x_r - \mu_r)'\right]\left[(x_s - \mu_s)(x_s - \mu_s)'\right]}} \tag{23}$$

where x_r is the query image distance vector and x_s is the distance vector of images included in the database.μ_r and μ_s are the means of the vectors x_r and x_s.

5. Experimental Results

To verify the retrieval performance of the proposed method, three different banknote image sets in the experiments are presented separately.

5.1. Banknote Image Database

The banknote image samples are scanned by contact image sensor with 200dpi.The samples are classified to three database described as follows:
(1). Database D1: the banknote image database D1 consists of 16000 images of RMB.The size of each image is 270×140.It has five main values which are 100,50,20,10,5 Yuan, and each value has four faces. So there are 20 classes in the D1.
(2). Database D2: the banknote image database D2 consists of 20000 images of USD.The size of each image is 270×140.It has six main values which are 100,50,20,10,2,1 Dollar,and each value has four faces. D2 has 24 classes totally.
(3). Database D3: the banknote image database D3 consists of 10000 images of EURO.The size of each image is 270×140.It has seven main values which are 500,200,100,50,20,10,5 euro-dollar, and each value has four faces.There are 28 classes in the D3.

5.2. Average Retrieval Accuracy

The combination of standard deviation and energy is used as feature of the banknote image. From Table1 to Table3, they provide a comparison of average retrieval accuracy for D1, D2 and D3 using feature sets (a)-(e) respectively.The results of accuracy indicate that the proposed method outperforms the other methods on each database. The main reason is that the RQWF provides complementary banknote image texture information to the QWT by the use of its orientation selectivity.The retrieval performance is evaluated in terms of the average rate of the recognition rate.Fig9(a), Fig9(b) and Fig9(c) show the comparison for D1, D2 and D3, respectively.It is clear that the proposed method is superior to the other method. The performance increased up to 98.10%, 98.98% and 98.16% respectively.

5.3. Banknote Image Retrieval Time

Table4 shows the time of feature extraction and search of the each database for given query banknote image.The simulation is performed in Matlab7.5 running on 3.0G.Hz CPU and 1.0 GB of RAM. The results show that the proposed method saves reasonable time compared with other methods.

6. CONCLUSION

A new banknote image retrieval method that using standard quaternion wavelet transform (QWT) and rotated quaternion wavelet transform jointly is proposed in this paper.The proposed method is shift invariant,which it inherits from DWT and DT-CWT and captures the diagonal texture information of banknote image clearly.SVM is used as classifier in the banknote retrieval system.The proposed method is verified on Database D1-D3. Experimental results on database D1 consisting of 16000 banknote images of RMB, database D2 consisting of 20000 banknote images of USD and database D3 consisting of 10000 banknote images of EURO indicate that the proposed method significantly improves the recognition rate from 78.79% to 91.22%, 74.08% to 94.62% and 76.44% to 88.78% respectively, over the other method.

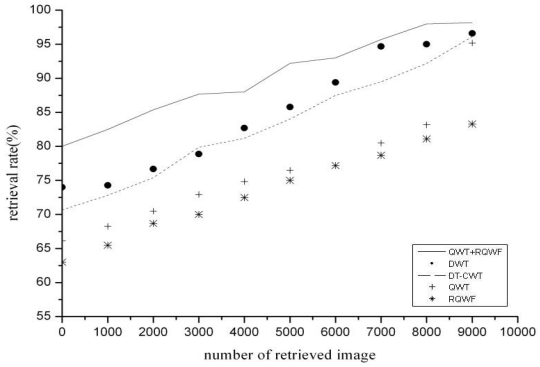

(a)

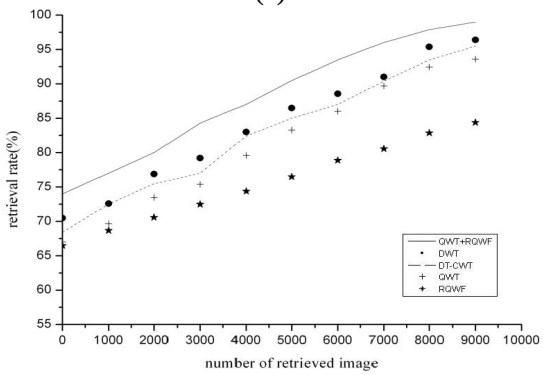

(b)

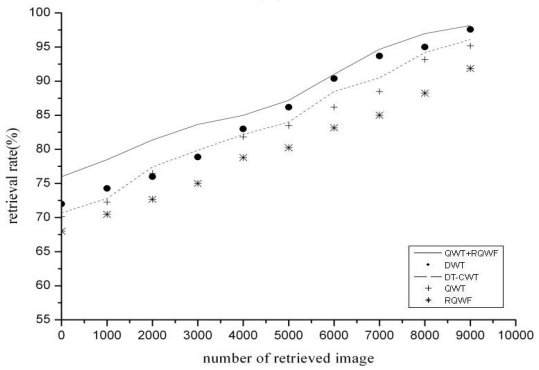

(c)

Fig. 9. Retrieval rate using different database,(a) D1,(b) D2,(c)D3.

Table 1. Average retrieval accuracy of RMB of the database D1 with energy and standard deviation as feature measure.

RMB	DWT	DT-CWT	QWT	RQWF	QWT RQWF
100	73.21%	69.39%	75.40%	73.28%	85.48%
50	74.68%	76.06%	83.07%	79.15%	89.72%
20	78.25%	75.45%	86.72%	83.52%	93.45%
10	82.14%	80.25%	85.48%	82.78%	95.27%
5	85.68%	81.65%	81.29%	80.86%	92.18%

Table 2. Average retrieval accuracy of USD of the database D2 with energy and standard deviation as feature measure.

USD	DWT	DT-CWT	QWT	RQWF	QWT RQWF
100	71.08%	76.09%	80.06%	77.45%	94.98%
50	72.35%	78.56%	81.35%	78.78%	92.87%
20	71.64%	79.14%	83.17%	82.58%	95.50%
10	76.03%	73.89%	78.84%	76.84%	95.96%
2	75.14%	72.75%	76.92%	75.28%	91.98%
1	78.24%	74.95%	75.97%	74.62%	96.45%

Table 3. Average retrieval accuracy of Euro of the database D3 with energy and standard deviation as feature measure.

EURO	DWT	DT-CWT	QWT	RQWF	QWT RQWF
500	74.28%	69.48%	72.18%	70.95%	83.69%
200	76.40%	72.15%	76.24%	73.28%	85.46%
100	77.36%	74.86%	74.48%	71.40%	88.49%
50	72.73%	73.28%	68.73%	70.36%	90.25%
20	80.03%	68.84%	73.46%	72.46%	92.51%
10	74.92%	73.48%	70.26%	69.50%	91.45%
5	79.38%	75.28%	76.85%	75.58%	89.58%

Table 4. Searching time of query banknote image.

Feature measure	DWT	DT-CWT	QWT	RQWF	QWT RQWF
Feature length	24	40	96	96	192
Extraction time	0.53s	0.68s	0.82s	0.78s	1.01s
query time	0.058s	0.065s	0.072s	0.073s	0.078s

Acknowledgments

This paper was partially supported by National Natural Science Foundation of China(60702032);

Harbin Special Funds for Technological Innovation Research(2009RFQXG208); Natural Science Foundation of Heilongjiang(QC2009C06);

References

1. Liu.F,Picard.R.W,"Periodicity,directionality,and randomness:wold features for image modeling and retrieval," *IEEE Trans. on Pattern Analysis and Machine Intelligence*, **18**, 722–733 (1996).
2. Manjunath.B.S,Ma.W.Y,"Texture features for browsing and retrieval of image data," *IEEE Trans. on Pattern Analysis and Machine Intelligence*, **8**, 837–842 (1996).
3. Xiangxun Chen,"Real wavelet transform-based phase information extraction method:theory and demonstrations," *IEEE Trans. on Industrial Electronics*, **56**, 891–899 (2009).
4. Antonino.D.J.A et al,"Feature extraction for the prognosis of electromechanical faults in electrical machines through the DWT," *International Journal of Computational Intelligence Systems*, **2**, 158–167 (2009).
5. Runyi Yu,"A new shift-invariance of discrete-time systems and its application to discrete wavelet transform analysis," *IEEE Trans. on Signal Processing*, **57**, 2527–2537 (2009).
6. T.Randen,J.H.Husoy,"Filtering for texture classification:A comparative study," *IEEE Trans. on Pattern Analysis and Machine Intelligence*, **21**, 291–310 (1999).
7. Andreopoulos.Y,Van der Schaar.M,"Incremental refinement of computation for the discrete wavelet transform," *IEEE Trans. on Signal Processing*, **56**, 140–157 (2008).
8. Jian-Da Wu,Chuang-Chin Hsu and Guo-Zhen Wu,"Fault gear identification and classification using discrete wavelet transform and adaptive neuro-fuzzy inference," *Journal of Expert Systems with Applications*, **36**, 6244–6255 (2009).
9. Do.M.N,Vetterli.M,"Wavelet-based texture retrieval using generalized Gaussian density and Kullback-Leiber distance," *IEEE Trans. on Image Processing*, **11**, 146–158 (2002).
10. Janney.P,Geers.G,"Texture classification using invariant features of local textures," *IEEE Trans. on Image Processing*, **4**, 158–171 (2010).
11. Charalampidis.D,Kasparis.T,"Wavelet-based rotational invariant roughness features for texture classification and segmentation," *IEEE Trans. on Image Processing*, **11**, 825–837 (2002).
12. Guangcan Liu,Zhouchen Lin and Yong Yu,"Randon representation-based feature descriptor for texture classificatoin," *IEEE Trans. on Image Processing*, **18**, 921–928 (2009).
13. J.L.Chen,A.Kundu,"Rotational and gray-scale transform invariant texture identification using wavelet decompositon and hidden markov model," *IEEE Trans. on Pattern Analysis and Machine Intelligence*, **16**, 208–214 (1994).
14. R.Manthalkar,P.K.Biswas,B.N.Chatterji,"Rotation and scale invariant texture features using discrete wavelet packet transform," *Journal of Pattern Recognition Letters*, **24**, 2455–2462 (2003).
15. Duncan D.Y.Po,Minh N.Do,"Directional multiscale modeling of images using the contourlet transform," *IEEE Trans. on Image Processing*, **15**, 1610–1620 (2006).
16. W.Selesnick,R.G.Baraniuk and N.G.Kingsbury,"The dual-tree complex wavelet transform," *IEEE Trans. on Processing Magazine*, **22**, 123–151 (2005).
17. Ioannidou.S,Karathanassi.V,"Investigation of the Dual-Tree Complex and Shift Invariant Discrete Wavelet Transform on Quickbird Image Fusion," *IEEE Trans. on Geoscience and Remote Sensing Letters*, **4**, 166–170 (2007).
18. E.B.Corrochano,"The theory and use of quaternion wavelet transform," *Journal of Mathematical Imaging and Vision*, **24**, 19–35 (2006).
19. Wai Lam Chan, Hyeokho Choi and Richard G.B,"Coherent multiscale image processing using dual-tree quaternion wavelets," *IEEE Trans. on Image Processing*, **17**, 1069–1082 (2008).
20. M.N.Do,M.Vetterli,"Pyramidal directional filter banks and curvelets," *Proc. IEEE Intl. Conf. on Image Processing*, **3**, 158–161 (2001).